**Current Biology, Volume *19***

# Supplemental Data

# Compression Regulates

# Mitotic Spindle Length by a

# Mechanochemical Switch at the Poles

**Sophie Dumont and Timothy J. Mitchison**

## Supplemental Experimental Procedures

### Spindle Thickness and Volume Estimates

Spindle thickness measurements were calibrated using FocalCheck ring stained beads (Invitrogen F-14806) of 5.90±0.05 μm diameter, placed in L-15 on a coverslip and pressed down with an agarose pad as described. Spindle thickness was measured before, during and after compression by taking *z*-stack images (every 200 nm). Spindle volume was estimated as that of an ellipsoid, $\frac{4\pi \cdot l \cdot w \cdot z}{3}$, with *l* being spindle half-length, *w* spindle half-width and *z* spindle half-thickness (note that normalized volumes in Fig. 2A are shape-independent). Although further work would be required to get a more accurate estimate of the absolute spindle thickness, relative spindle thickness measurements are sufficient for meaningful spindle volume comparison.

### Perturbation Strength

Based on previous Young's modulus measurements [1, 2] and observed cellular parameters (original cell area, and fractional cell thickness change), we estimate ~100 nN are applied to the cell. The exact amount of force applied to the spindle is not known (because the rest of the cell also deforms), but the perturbation is applied isotropically in the *xy*-plane, and thus width and length responses can be compared. Perturbations were grouped in two categories: gentle compression, that caused spindle length to increase by 0-40%, and strong compression, that caused spindle length to increase by >40%. Gentle compression was completely reversible when the agarose pad was rapidly (~10 s) removed: the spindle returned to its original shape and size, keeping its architecture intact, and cells entered anaphase at any time during this perturbation. Strong compression was typically not fully reversible when the agarose pad was rapidly removed, and cells typically did not enter anaphase during or after such a perturbation. In most cases the cell rounded up quickly. If strong compression was removed more slowly (over >>10 s), the spindle responded more reversibly (Fig. 1E, Movie S2) and anaphase entry sometimes followed (Fig. 3C).

**Image Analysis**

For cell and spindle width and length analysis, phase and fluorescence images were analyzed with Metamorph by manual feature identification at each time frame. Data from the few largest compression perturbations where poles and centrosomes detached were not included. Analysis was stopped upon anaphase entry. Time series data were further analyzed in Matlab (The Mathworks, Inc.) for expansion and contraction parameters. The velocity was calculated as the ratio of distance change to duration of response for individual spindles, thus representing the mean velocity for the entire response. Correlation analysis was performed using Matlab's *corrcoef* function. For k-fiber cross-sectional intensity analysis, the brightest z-plane was chosen, maximum intensity of a 5-pixel linescan across the fiber measured and nearby background subtracted. This was repeated over several EGFP-α-tubulin k-fibers per spindle. Cross-sectional fiber intensities were averaged for non-compressed and compressed spindles and then compared, and few images were acquired between measurements to minimize photobleaching. For total tubulin mass measurements, EGFP-tubulin *z*-stack intensities were integrated and background integrated and subtracted; compression caused extreme background variations, making quantitative measurements difficult. For inter-kinetochore distance and kinetochore velocity analysis, a Matlab program, SpeckleTracker (Xiaohu Wan, UNC Chapel Hill), was used to identify and track EYFP-cdc20 kinetochores over time. Briefly, kinetochores were detected by thresholding a smoothed image and their centroid positioned with sub-pixel accuracy via a two-dimensional Gaussian fit. Tracking was performed by finding the nearest kinetochore in the next frame. Poles were not automatically detected. A home-written Matlab program created kinetochore pairs, found turnaround points in oscillations, and measured inter-kinetochore distance and velocity, the latter defined as distance travelled per half-cycle divided by duration of that half-cycle (a half-cycle is the time between turnaround points). We only tracked kinetochore pairs oscillating with high amplitude near the center of the spindle, whose motion was not obviously impeded by that of neighboring chromosomes. For tubulin sliding velocity analysis, we used the kymograph function in Metamorph to measure the velocity of the activated tubulin population with respect to the metaphase plate.

**Supplemental References**


1. Caille, N., Thoumine, O., Tardy, Y., and Meister, J.J. (2002). Contribution of the nucleus to the mechanical properties of endothelial cells. Journal of Biomechanics *35*, 177-187.
2. Matzke, R., Jacobson, K., and Radmacher, M. (2001). Direct, high-resolution measurement of furrow stiffening during division of adherent cells. Nature Cell Biology *3*, 607-610.

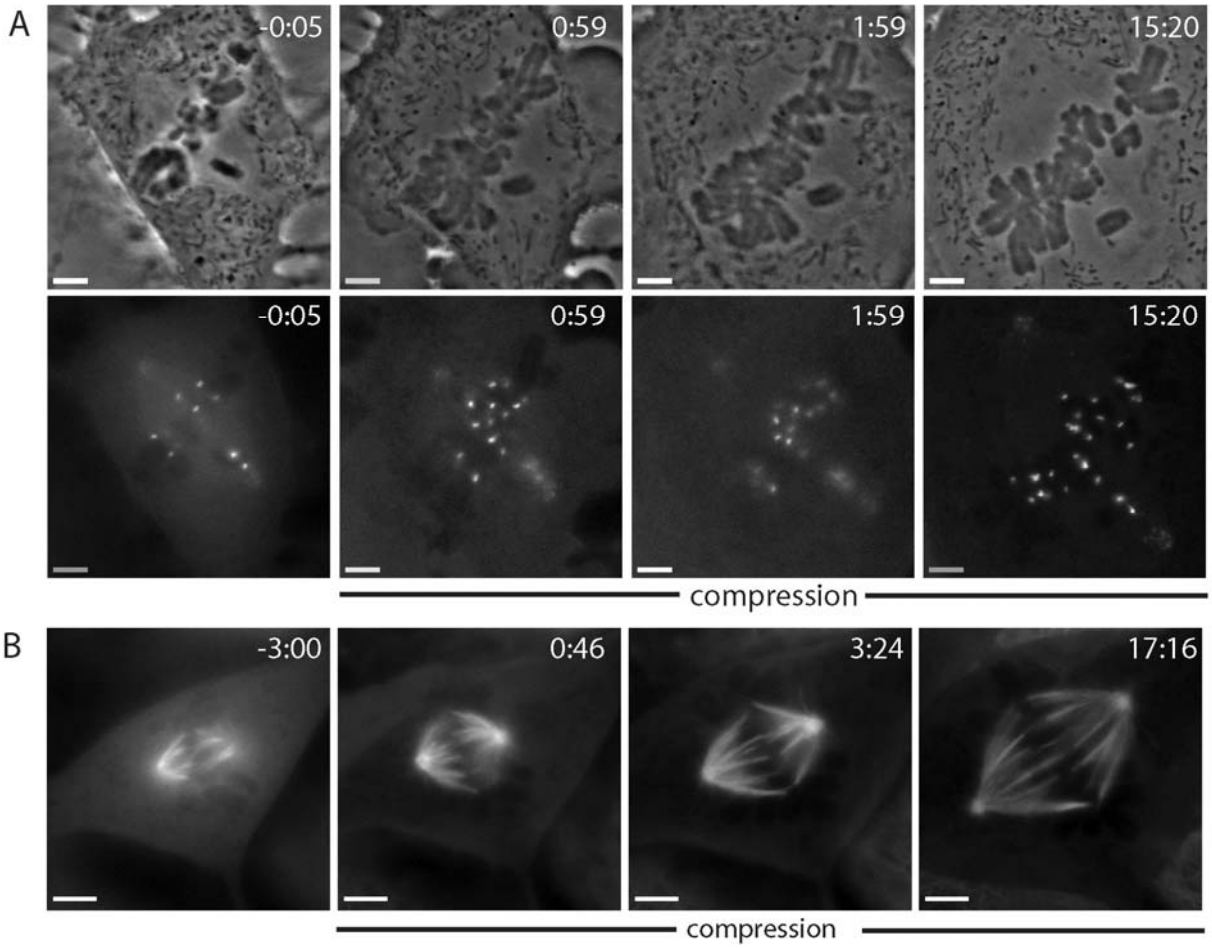


**Figure S1. A Compressed Mitotic Spindle Is Rescaled to Twice Its Original Size by Increasing the Length of K-Fibers**

Phase contrast and fluorescence imaging of a compressed spindle doubling in length in a Ptk2 EYFP-cdc20 cell (A) (note bleb at 0:59), and in a Ptk2 EGFP-α-tubulin cell (B) (note k-fiber pivoting by 0:46). Compression started at 0:00 (min:s) and scale bar corresponds to 5 μm.

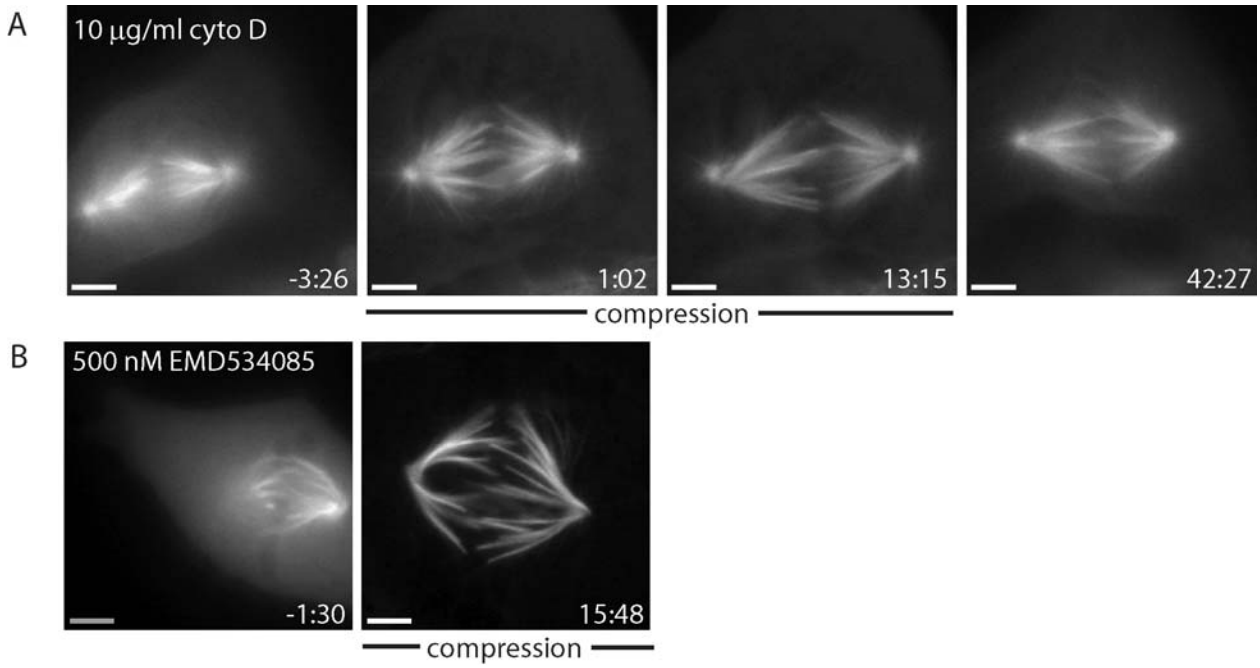


**Figure S2. Spindle Elongation Is Driven by Forces Internal to the Spindle that Are Kinesin-5 Independent**

Spindle being compressed in 10 μg/ml cytochalasin D (A) (release at 28:00), which depolymerizes actin, and 500 nM EMD534085 (B), which inhibits kinesin-5. Ptk2 EGFP-α-tubulin cells, compression started at 0:00 (min:s) and scale bar corresponds to 5 μm.

**Table S1. Correlation Analysis between Different Observables of Cell and Spindle Responses during Both Compression (Expansion) and Decompression (Contraction)**

| 1st Variable | 2nd Variable | Correlation Coefficient | p Value |
|---|---|---|---|
| Spindle Expansion | | | |
| $\Delta W$ | $\Delta CW$ | 0.79 | $7.2 \times 10^{-8}$ |
| $\Delta L$ | $\Delta W$ | 0.77 | $2.6 \times 10^{-7}$ |
| Spindle area increase | Cell area increase | 0.72 | $3.5 \times 10^{-6}$ |
| Spindle Contraction | | | |
| $\Delta W$ | $\Delta CW$ | 0.78 | $1.8 \times 10^{-7}$ |
| $\Delta L$ | $\Delta W$ | 0.80 | $5.2 \times 10^{-8}$ |
| Spindle area increase | Cell area increase | 0.90 | $4.3 \times 10^{-12}$ |

Change in spindle length ($\Delta L$), spindle width ($\Delta W$), and cell width ($\Delta CW$).